ACS OMEGA

http://pubs.acs.org/journal/acsodf

Article

ZnO@Polyvinyl Alcohol/Poly(lactic acid) Nanocomposite Films for the Extended Shelf Life of Pork by Efficient Antibacterial Adhesion

Luoyan Duan, Feiyi Yan, Lei Zhang, Bo Liu, Yichi Zhang, Xinyuan Tian, Zhaoping Liu, Xiaodan Wang, Shuaiyu Wang, Jijing Tian, Huihui Bao,* and Tianlong Liu*

Cite This: *ACS Omega* 2022, 7, 44657−44669

Read Online

ACCESS | Metrics & More | Article Recommendations | Supporting Information

ABSTRACT: The proliferation of microorganisms is an important reason for meat spoilage and deterioration. Freezing and packaging by polymer films and preservatives are commonly used to preserve meat. While the energy consumption of freezing is very big, the polymer films made by petroleum bring up heavy environmental pressure. In the present study, biodegradable antibacterial ZnO@PLA (ZP) and ZnO@PVA/PLA (ZPP) nanocomposite films used as food packaging have been synthesized by the solvent evaporation method and coating method, respectively. Compared with films without ZnO NPs, ZP and ZPP both had long-term bacteriostasis for 24 and 120 h at temperatures of 25 and 4 °C, respectively. Moreover, the antibacterial effect showed positive relevance with the increase of the ZnO NP concentration. In addition, the antibacterial effect of ZPP was better than that of ZP in the same condition. Scanning electron microscopy showed that the numbers of methicillin-resistant staphylococcus aureus (MRSA) on ZP and ZPP were significantly reduced compared to that in the blank film, and ZPP caused the morphology of MRSA to change, which means that the antibacterial mechanism of ZP and ZPP composite films might be related to antibacterial adhesion. In conclusion, ZPP films have great potential to be regarded as the candidate of food packing to extend the shelf life of pork.

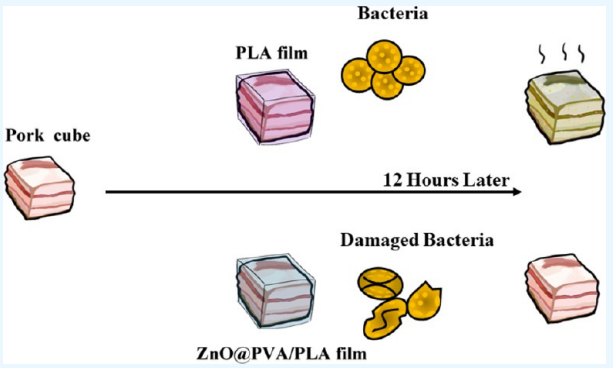

INTRODUCTION

Considering the increasing public interest in an increased shelf life of meat to ensure long-distance transportation, the usage of active packing, using nanotechnology to improve the quality and safety of food, is increasing.[1] Numerous methods have been developed to extend the shelf life, including the use of a natural plant extract compound coated on the packing paper for antibacterial effects. However, the volatile component in it could affect the odor and quality of meat.[2] Recently, an increasing number of studies have been carried out on the application of nanoscale inorganic matter in smart packaging systems for food. Food packing with the elements of nanomaterial elements provided improved physical performances, durability, barrier properties, and biodegradation. Moreover, the nanoscale antibacterial material has a high ratio of surface area to mass, which ensures better antibacterial properties.[3] Thus, nanomaterials have high potential for use as additives in active packing to extend the meat shelf life.

Poly(lactic acid) (PLA) has high potential for use in food packaging due to its biocompatibility, biodegradability, and nontoxicity.[4,5] In addition, PLA can be easily modified for provision of desired characteristics. The flexibility and crystallization properties of PLA could be enhanced by adding zinc oxide nanoparticles (ZnO NPs).[6,7] ZnO@PLA (ZP) nanocomposites exhibit good antibacterial performances.[8−10] ZnO NPs have been defined as a generally recognized as safe material by the US Food and Drug Administration.[11] The excellent antibacterial properties make them superior for various applications. The minimum inhibitory concentrations of the ZnO NPs, with a size of approximately 5 nm, are 0.0782 and 0.3125 mg/mL against *Staphylococcus aureus* and *E. coli*, respectively.[12] ZnO NP-loaded nanomaterials have excellent antibacterial activities. Ding et al[13] used ZnO NPs in situ loaded on palygorskite and introduced the composite into a chitosan/gelatin film to form an antibacterial packing film. Roberto Pantani et al reported that the ZP nanocomposite exhibited significant antimicrobial properties compared to a PLA film.[5] Similarly, the ZP nanocomposite fabricated by Murariu et al. exhibited a high ability to inhibit the growth of *S. aureus* and *Klebsiella pneumoniae*.[14] However, many studies have been

Received: May 15, 2022
Accepted: November 8, 2022
Published: November 28, 2022

https://doi.org/10.1021/acsomega.2c03016
ACS Omega 2022, 7, 44657−44669

focused on the results, while the antibacterial mechanism of ZnO NPs has not been elucidated.

Polyvinyl alcohol (PVA) is a surface-stabilizing agent that can reduce the size of ZnO NPs. Stankovic et al. revealed that compared to other groups, ZnO NPs/PVA exhibited the largest specific surface area and the smallest particle size, which has been regarded as the main reason for the highest antibacterial activity.[15] Antibacterial adhesion is a significant property in inhibition of bacterial colonization and proliferation. For example, Klemm et al. reported that the adhesion of both *S. aureus* and *Candida glabrata* to a polythiourethane matrix coated with ZnO NP fillers was decreased. Moreover, the number of bacterial adhesions was negatively correlated with the concentration of ZnO NPs.[16] Therefore, it is reasonable to speculate that the combination of ZnO NPs and PVA could enhance the antibacterial performance of PLA films and that the usage of ZnO NPs could hinder the bacterial adhesion to the PLA. Nevertheless, the antibacterial effect of ZnO NPs/PVA as a surface-coating agent on a PLA film and comparison of the antibacterial effects between the traditional ZP and novel ZnO@PVA/PLA (ZPP) nanocomposites have not been extensively studied. In addition, no extensive studies have been carried out on the influences of several factors on the shelf life considered simultaneously, such as the concentration of ZnO NPs[17,18] and storage temperature.[19]

In this study, we tested two methods with mixing directly inside the PLA packaging film as a nanocomposite and applied ZnO@PVA on the surfaces (nano-coatings) of PLA films. ZnO@PLA nanocomposites obtained by a solvent evaporation method (ZP) and ZnO@PVA/PLA nanocomposites obtained by a coating method (ZPP) were successfully synthesized. The antibacterial effects of ZP and ZPP on pork purchased from the market with different concentration gradients at various storage times at 4 and 25 °C were evaluated. According to the optimal conditions at 25 °C, an experiment on the antibacterial effects of the two types of nanocomposites on methicillin-resistant staphylococcus aureus (MRSA) was carried out. Scanning electron microscopy (SEM, HITACHI, Japan) images were acquired to analyze the performances of ZP and ZPP in antibacterial adhesion. The sub-acute toxicity of ZnO NPs was assessed after oral uptake to investigate the application potentials of the nanocomposites.

MATERIALS AND METHODS

Materials. PLA was purchased from Nature Works LLC (USA). PVA was purchased from Sigma-Aldrich (St. Louis, MO, USA). Pork was purchased from Beijing MerryMart Chain Commerce Co. Ltd. (Beijing, China). Nutrient agar was purchased from Coolaber Company (Beijing, China). All other reagents and chemicals used in this study were of analytical grade.

Preparation of ZnO NPs. The ZnO NP synthesis has been described.[20] 2.75 g of zinc acetate and 1 g of dimethyl sulfone were added to 75 mL of methanol, and then, the solution was quickly heated to 65 °C and sustained for at least 1 h. 1.47 g of hydroxide potassium was thoroughly dissolved in 25 mL of methanol, which was added to the above solution at 1 drop/2 s with a peristaltic pump. This reaction lasted for 2 h to obtain the final reaction product.

Characterization of ZnO NPs. Transmission electron microscopy (TEM, HITACHI H-7500, Japan) samples were prepared on carbon-coated copper grids. TEM measurements on the ZnO NPs after drying were performed at an accelerating voltage of 120 kV.[21] X-ray diffraction (XRD, Rigaku Ulima IV, Japan) patterns were acquired using Ni-filtered Cu Kα radiation with a wavelength of 1.5408 Å in a wide-angle 2θ region of a 20 to 70° scale to confirm the crystalline structure of the ZnO NPs.[22] In addition, the antibacterial effect of ZnO NPs against *E. coli* (ATCC25922) was estimated.[20]

Synthesis of the ZP Film. The synthesis has been described in ref 23. 0.4 g of PLA was dissolved into 18, 19, 19.5, and 19.75 mL of dichloromethane and stirred for 2 h, respectively. 2, 1, 0.5, and 0.25 mL of 10 mg/mL ZnO NPs were then added to the above solution and stirred with magnetic stirrers until all NPs were completely mixed. The solution was then poured over a polytetrafluoroethylene plate (10 cm × 10 cm). After the dichloromethane was evaporated completely, composite membranes were peeled off and placed into a vacuum dryer for a constant temperature drying for 12 h. Therefore, 5, 2.5, 1.25, and 0.625% ZP films were prepared. They are abbreviated as ZP-5%, ZP-2.5%, ZP-1.25%, and ZP-0.625%, respectively.

Synthesis of the ZPP Film. The PLA films were synthesized as mentioned above. Then, 10, 5, 2.5, and 1.25 mg/mL of ZnO NPs were ultrasonically dispersed for 2 h in 1% PVA, respectively, which was previously completely dissolved in distilled water. In addition, 0.1 mL of the above solution was coated on the surface of the synthesized PLA films. Accordingly, 5, 2.5, 1.25, and 0.625% ZPP films were prepared, denoted as ZPP-5%, ZPP-2.5%, ZPP-1.25%, and ZPP-0.625% in short, respectively.

Characterization of ZP and ZPP Films. The morphological and compositional analyses of all the samples were carried out using an SEM−energy-dispersive X-ray spectroscopy instrument (JEOL-JSM-8040, Tokyo, Japan). All ZP and ZPP films were analyzed by inductively coupled plasma mass spectrometry (ICP−MS, 8800, Agilent Technologies, USA) to determine the zinc contents on the films.[24]

Migration Test for the ZP Composite. This test was guided by China's national standard GB/T5009.156−2003 and European Union Standard (EU) no. 10/2011. To be specific, 65% (v/v) ethanol, 4% (w/v) aqueous acetic acid, N-hexane, and distilled water were applied to simulate the effect of alcoholic food, acidic food, and fat- and water-based food, respectively. 5 cm × 5 cm ZnO NP/PLA films with a concentration of 2% were added into the blue-mouth bottles equipped with the above simulation liquids for 10 days at 4 and 25 °C, separately. Finally, all samples were analyzed by ICP−MS to detect the zinc content migrated from the film.[24]

Bacterial Inhibition Test on Pork. Pork used for this research purchased from the market was cut into cubes (2 cm × 2 cm ×2 cm) after washing with water. All of the samples of nanocomposites were sterilized with an ultraviolet lamp for at least 20 min before application. The pork cubes were then wrapped by ZP and ZPP films with the concentrations of 5, 2.5, 1.25, and 0.625%. The pork cubes cloaked by films were then placed into the 5 mL Eppendorf tubes previously autoclaved for 30 min. The Eppendorf tubes with samples were then separately placed at the sterile incubator shakers at 4 and 25 °C for different periods. We sampled at 0, 2, 4, 6, 12, and 24 h in the 25 °C groups, while, for the 4 °C groups, besides the periods mentioned above, we sampled every 12 to 120 h. In the end, the colony-forming unit (CFU) of each sample was determined by the colony-counting method.[25,26]

Assessment of the Bacterial Inhibition Ability of Nanocomposites against MRSA. The process of this section was similar to that of the former experiment. The pork cubes

https://doi.org/10.1021/acsomega.2c03016
ACS Omega 2022, 7, 44657−44669

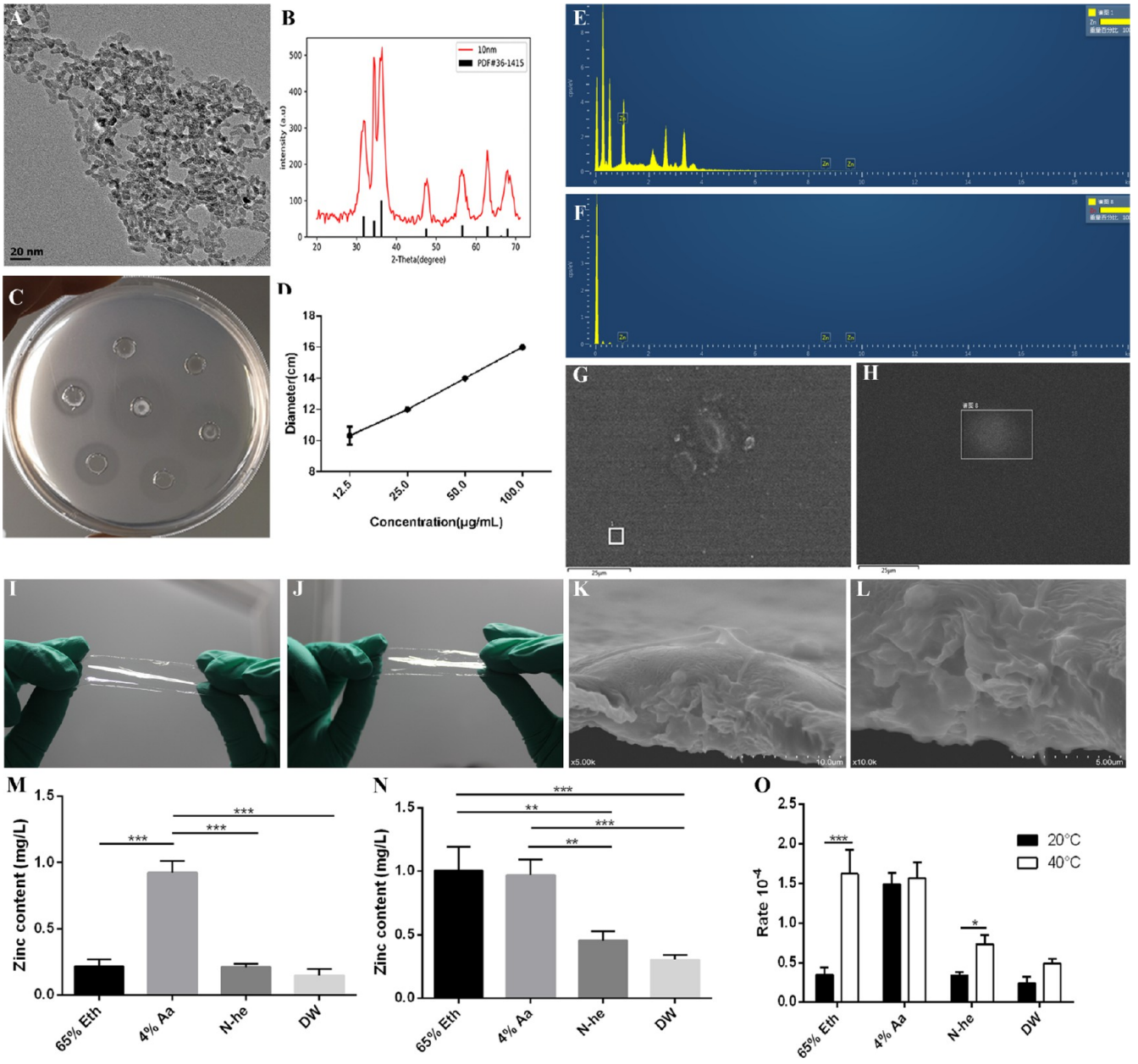

Figure 1. Characterization of ZnO NPs, ZnO NP films, and migration of Zn from the ZP film into four different kinds of food simulants. (A) TEM image of ZnO NPs. (B) XRD patterns of ZnO NPs. (C) Photograph of the inhibition zone of ZnO NPs to *E. coli*. (D) Measurement of the inhibition zone of ZnO NPs to *E. coli*. (E) EDS image of ZPP films.(F) EDS image of ZP films. (G) ZnO NP distribution of ZPP films. (H) ZnO NP distribution of ZP films. (I) Profile display of ZPP films. (J) Profile display of ZP films. (K) SEM image of ZPP films. (L) SEM image of ZP films. (M) Migration of Zn from the ZP film into 65% (v/v) ethanol, 4% (w/v) aqueous acetic acid, N-hexane, and distilled water for 10 days under 20 °C. (N) Migration of Zn from the ZP film into 65% (v/v) ethanol, 4% (w/v) aqueous acetic acid, N-hexane, and distilled water for 10 days under 40 °C. (O) Comparison of the Zn content of migration from the ZP film into 65% (v/v) ethanol, 4% (w/v) aqueous acetic acid, N-hexane, and distilled water for 10 days between 20 and 40 °C.

were sterilized with an ultraviolet lamp for approximately 20 min before use. Besides, the pork cubes were soaked into an MRSA solution with 1.8×10^2 cfu for 30 s. The best antibacterial effect conditions with different concentrations of the films at 25 °C were chosen for further assessment. They were 1.25% ZP and 0.625% ZPP at 4 h, 2.5% ZP and 1.25% ZPP at 6 h, and 5% ZP, 2.5% ZPP, and 5% ZPP at 12 and 24 h, respectively.

SEM Analysis of Bacterial Adhesion. The films (1×1 cm^2) were soaked in a 10 mL nutrient broth medium, which contained approximately 5×10^7 cfu of MRSA. After 4 h of incubation at 37 °C, the films were washed three times in sterile phosphate-buffered saline to remove the unattached bacteria and fixed with 2.5% glutaraldehyde overnight. The samples were then fixed in 1% osmic acid and dehydrated with gradient alcohol (30.50, 70, 80, 90, and 100%) for 15 min. The films were then dried in a drying oven and carefully stuck on a conductive adhesive. The films were gold-coated at 30 mA for 1 min and imaged by using a scanning electron microscope (ZEISS Sigma 300) at magnifications of 1000× and 8000×.

Animals and Treatment. Thirty female pathogen-free Institute of Cancer Research (ICR) mice (age: 6 weeks) were provided by Beijing Vital River Laboratory Animal Technology

https://doi.org/10.1021/acsomega.2c03016
ACS Omega 2022, 7, 44657−44669

Co. Ltd. The animal experiment was performed strictly according to the guidelines approved by the China Agricultural University Animal Centre Laboratory, China. The ICR mice received ZnO NPs dispersed in distilled water by intragastric administration at different levels of 63 to 200 mg/mL, determined by the maximum tolerated dose by preliminary studies.[27] Mice that received distilled water by intragastric administration were used as a control. Five mice were raised in one cage as one group. After intragastric administration, the symptoms and mortality of each mouse were recorded carefully every day. On the 14th day after the intragastric administration, all mice were sacrificed, and the serum and organs were sampled. The major organs were utilized for a histological examination with standard techniques.

Blood Routine Examination and Serum Biochemical Analysis. A hematology analysis was performed using standard collection techniques. There were several standard markers selected for further analysis: red blood cells (RBCs), hemoglobin (HGB), hematocrit (HCT), mean corpuscular volume (MCV), mean corpuscular hemoglobin (MCH), mean corpuscular hemoglobin concentration (MCHC), white blood cells (WBCs), and platelets (PLTs). Blood samples were centrifuged at 3000 rpm for 20 min to separate the serum. There were two important indicators chosen to assess the hepatic function: alanine aminotransferase (ALT) and aspartate aminotransferase (AST). Blood urea nitrogen (BUN) and creatinine (CREA) were used to determine the nephrotoxicity. A biochemical autoanalyzer (Type 7170, Hitachi, Japan) was used to evaluate all parameters.

Statistical Analysis. The data were represented as means ± standard deviations. An analysis of variance was carried out using GraphPad Prism version 8.0 (GraphPad Inc, San Diego, CA, USA). Duncan's multiple range test methods were used to compare means for each test, with statistical significance defined at a level of $p < 0.05$.

RESULTS AND DISCUSSION

Synthesis and Characterization of ZnO NPs. Figure 1A shows the TEM image of the synthesized ZnO NPs. The ZnO NPs were spherical, with an average size of approximately 10 nm. The XRD patterns reflect the existence of ZnO NPs.[28] Figure 1B shows that the diffraction peaks of the ZnO NPs are consistent with the Joint Committee on Powder Diffraction Standards (JCPDS) PDF#36−1415.The antibacterial ability of ZnO NPs is related to their size.[20] Figure 1C shows various inhibition zones after the treatment with different concentrations of ZnO NPs against *E. coli*. As can be seen from Figure 1D, the antibacterial effect of the ZnO NPs against *E. coli* exhibited presented a concentration dependence. Moreover, at the lowest concentration of 12.5 μg/mL, the antibacterial ability of the ZnO NPs was still good.

Characterization of the ZnO NP Films. Energy-dispersive X-ray spectroscopy (EDS) elemental analysis results of the two films are shown in Figure 1E,F. Besides Si, Al, and O signals, signals of Zn were also detected in the ED spectra. The detailed EDS elemental mapping of the nanocomposites shown in Figure 1G,H confirmed the Zn element distribution on the surfaces of the films. The two films were clear, thick, and transparent (Figure 1I,J). Figure 1K,L shows that the thickness of this type of film was approximately 5 μm. Even though the amount of ZnO NPs on the film could not be determined, the Zn contents of the films detected by ICP−MS could demonstrate the existence of ZnO NPs (Table 1). According to Table 1, the effective concentration of ZnO NPs on the ZP film was lower than that on the ZPP film when the same concentration of ZnO NPs was added.

Table 1. Comparison of Zn Content Detected by ICP−MS between ZP and ZPP Composite Films

groups	added ZnO NPs concentration	detected Zn content	detectable rate(%)	
PLA	0	0		
ZP	5%	3.8%	76%	a
ZPP	5%	4.6%	92%	b
ZP	2.5%	1.91%	76.4%	a
ZPP	2.5%	2.31%	92.4%	b
ZP	1.25%	0.9%	72.4%	a
ZPP	1.25%	1.1%	88%	b
ZP	0.625%	0.45%	72%	a
ZPP	0.625%	0.56%	90%	b

In addition, the physical properties of the two films, such as water vapor transmission, oxygen permeability, light transmission, and mechanical properties, were evaluated (Figure S1 and Table S1). The relative results demonstrate that films synthesized in this research have good physical properties compared to the PLA film and are consistent with other studies.[8,29,30]

Migration of ZnO NPs from the ZP Films. The ZP film possesses antibacterial characteristics owing to various factors including the migration of ZnO NPs from the film. The ZnO NPs could compromise the lipids and proteins of bacteria and accelerate their death.[31] Therefore, it is essential to investigate the fate of the migration of the ZP film. Figure 1M shows that the migration of Zn from the ZP film into a 4% (w/v) aqueous acetic acid for 10 days at 20 °C is significantly higher than the Zn contents detected in the three other types of food simulants under the same conditions ($P < 0.001$), while there is no difference among 65% (v/v) ethanol, N-hexane, and distilled water. According to Figure 1N, the migrations of Zn from the ZP film into 65% (v/v) ethanol and 4% (w/v) aqueous acetic acid for 10 days at 40 °C are significantly higher than those for N-hexane and distilled water, respectively ($P < 0.001$). As shown in Figure 1O, the migrations of Zn from the ZP film into 65% (v/v) ethanol and N-hexane for 10 days at 40 °C are significantly higher than those at 20 °C ($P < 0.05$), while the migrations of Zn for the 4% (w/v) aqueous acetic acid and distilled water do not seem to be correlated with the temperature ($P > 0.05$). The reason is mainly because the increase of temperature accelerates the molecular thermal motion in the alcoholic and oil food stimulants, allowing Zn ions to migrate out of the PLA polymer.[32,33] These results demonstrate that the temperature should be considered for ZP film applications regarding storage of alcoholic foods and oily foods, consistent with other reports.[34−38]

Bacterial Inhibition Test on the Two Films under Natural Conditions at 25 °C. The consumption of animal foods, mostly pork, has rapidly increased.[39] The storage temperature of pork is regarded as one of the important factors that influence the quality and shelf life due to the relation with the properties of bacterial growth.[19] To estimate the antibacterial ability of the ZP film at 25 °C, a pork cube was wrapped with ZP or ZPP films with different concentrations of ZnO NPs and packaged in 5 mL Eppendorf tubes previously autoclaved for 30 min. Then, the Eppendorf tubes with samples

https://doi.org/10.1021/acsomega.2c03016
ACS Omega 2022, 7, 44657−44669

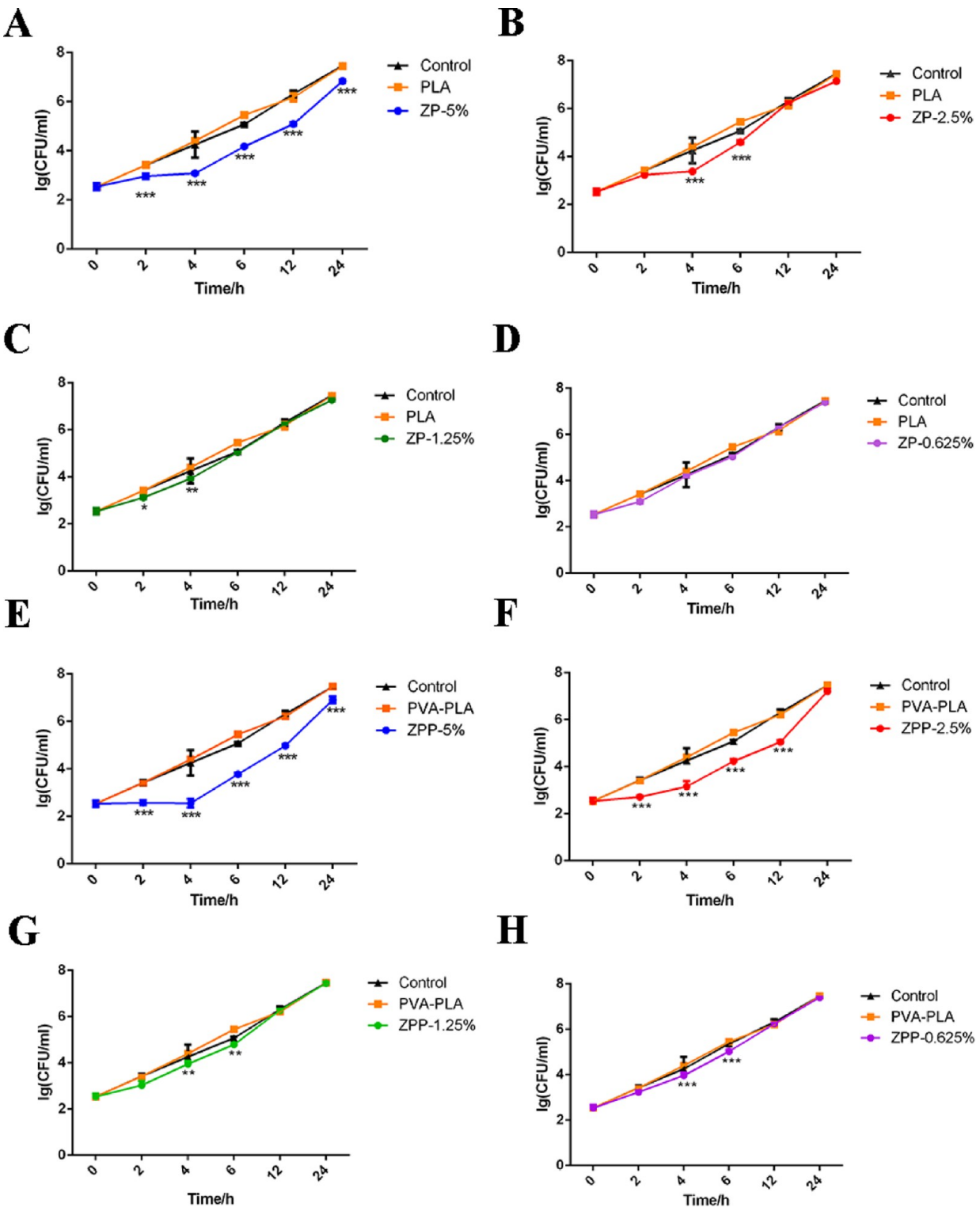

Figure 2. Bacterial counts in wrapped pork samples with different concentrations of ZP and ZPP films during different periods at 25 °C. (A−D) Bacterial counts in wrapped pork samples with 5, 2.5, 1.25, and 0.625% ZP films during different periods at 25 °C, respectively. (E−H) Bacterial counts in wrapped pork samples with 5, 2.5, 1.25, and 0.625% ZPP films during the storage time at 25 °C, respectively.

were separately placed in sterile incubator shakers at 25 °C for different periods. According to Figure 2A, compared to the other counterparts, the ZP-5% composite group exhibited the slowest bacterial count curve, and its bacterial counts were always significantly lower than those of the blank and single PLA in the period of 2 to 24 h. However, the bacterial counts of the ZP-2.5% and ZP-1.25% composite groups were significantly lower than those of their counterparts in the period of 4 to 6 h and 2 to 4 h (Figure 2B,C). Figure 2D shows that the bacterial counts of ZP-0.625% were not significantly different from those of the blank and single PLA during the recorded periods. Accordingly, the antibacterial ability of the ZP film at 25 °C exhibited a concentration-dependent trend. The ZP-5% composite could be regarded as the most effective film against bacteria in pork. The

https://doi.org/10.1021/acsomega.2c03016
ACS Omega 2022, 7, 44657−44669

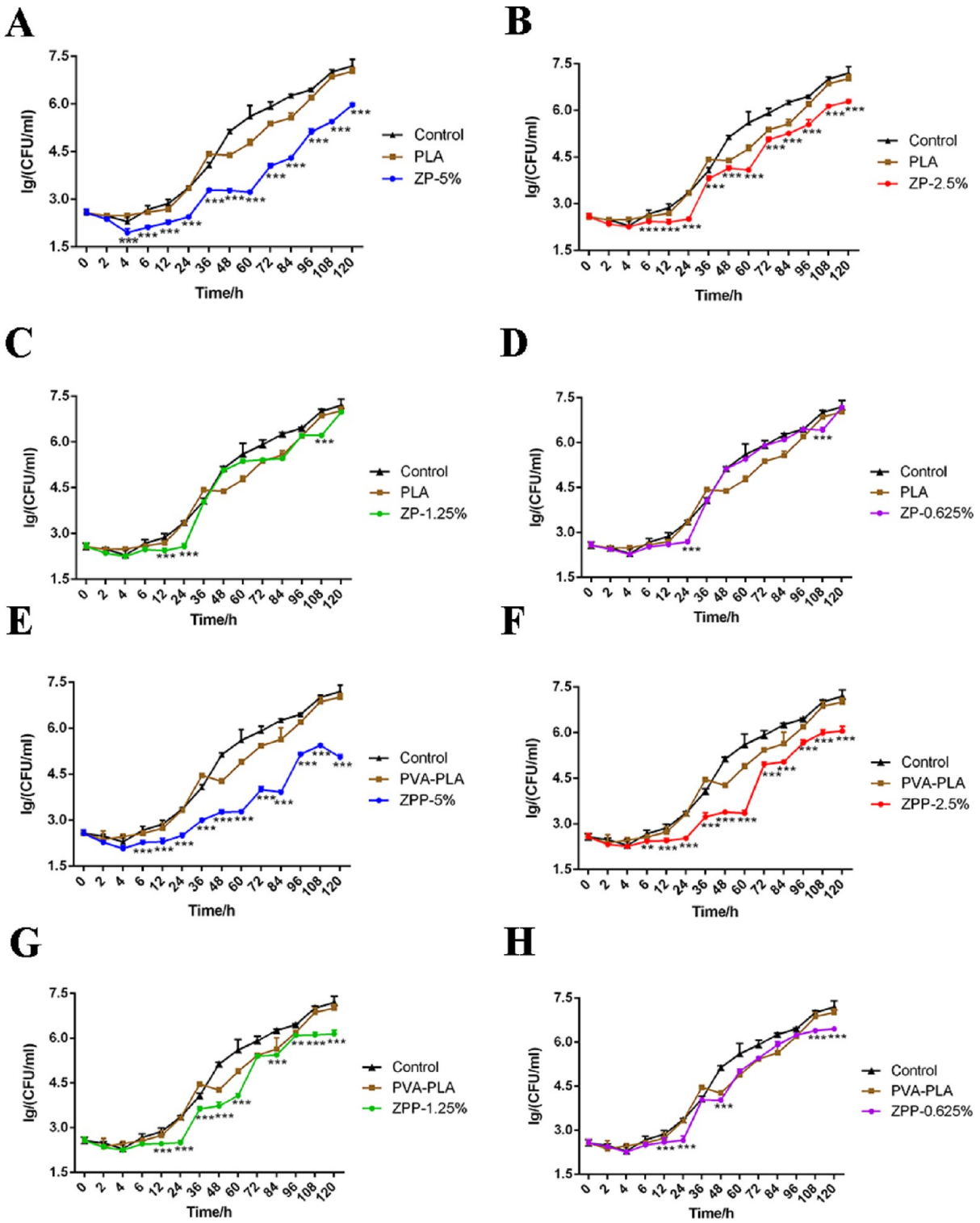

Figure 3. Bacterial counts in wrapped pork samples with different concentrations of ZP and ZPP films during different periods at 4 °C. (A−D)Bacterial counts in wrapped pork samples with 5, 2.5, 1.25, and 0.625% ZP films during different periods at 4 °C, respectively. (E−H) Bacterial counts in wrapped pork samples with 5, 2.5, 1.25, and 0.625% ZPP films during the storage time at 4 °C, respectively.

minimum effective concentration was obtained for ZP-1.25% at 4 h, ZP-2.5% at 6 h, and ZP-5% at 12 and 24 h. Thus, they were chosen as optimal to assess the antibacterial activity of ZP films against MRSA at different periods at 25 °C. The antibacterial abilities of the ZPP films at 25 °C were also investigated. According to Figure 2E,F, the bacterial counts of the ZPP-5% and ZPP-2.5% nanocomposites were always significantly lower than those of the blank and single PLA in the periods of 2 to 24 h and 2 to 12 h. In the period of 4 to 6 h, the bacterial counts of both ZPP-1.25% and ZPP-0.625% films were significantly lower than those of their counterparts (Figure 2G,H). Overall, the concentration-dependent trend has also been observed. The minimum effective concentrations at 4, 6, 12, and 24 h were obtained for ZPP-0.625%, ZPP-1.25%, ZPP-2.5%, and ZPP-5%,

https://doi.org/10.1021/acsomega.2c03016
ACS Omega 2022, 7, 44657−44669

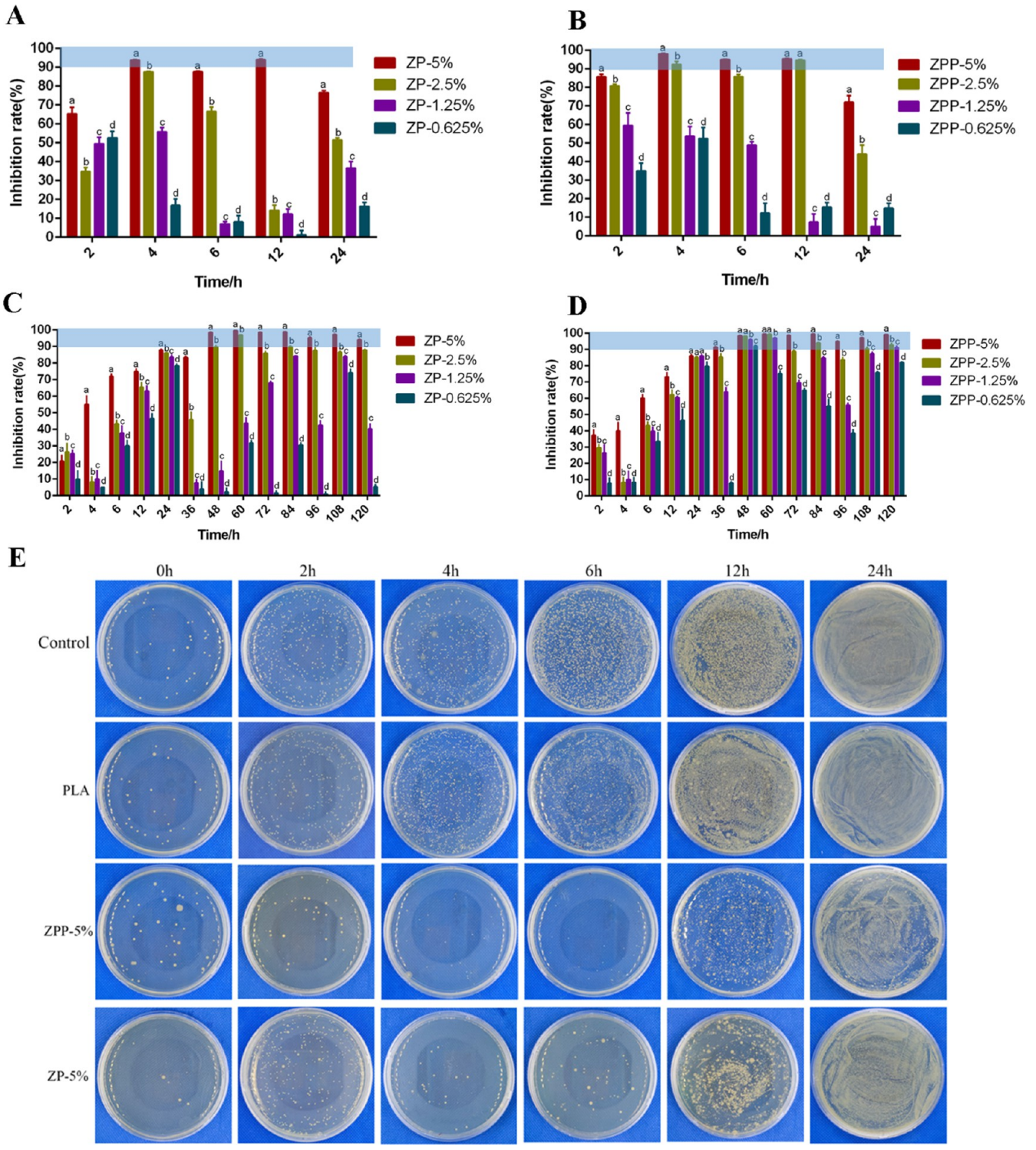

Figure 4. Total inhibition rate in wrapped pork samples with different concentrations of nanocomposites in different methods during the storage time at 25 and 4 °C and the colony formation of the wrapped pork samples with different concentrations of nanocomposites in different methods during the storage time at 25 °C. Shaded areas represent bacterial inhibition rates which are more than 90%. (A) Total inhibition rate in wrapped pork samples with different concentrations of ZP films during the storage time at 25 °C. (B) Total inhibition rate in wrapped pork samples with different concentrations of ZPP films during the storage time at 25 °C. (C) Total inhibition rate in wrapped pork samples with different concentrations of ZP films during the storage time at 4 °C. (D) Total inhibition rate in wrapped pork samples with different concentrations of ZPP films during the storage time at 4 °C. (E) Comparison of the formation of bacterial colonies of pork samples coated with ZP or ZPP films at 25 °C.

respectively. Therefore, we selected these conditions as optimal to assess the antibacterial activities of ZPP films against MRSA at different periods at 25 °C.

Bacterial Inhibition Test on Films in Natural Conditions under 4 °C. The antibacterial abilities of the nanocomposites synthesized by the two different methods were also evaluated at 4 °C. Regarding the ZP films, as shown in

https://doi.org/10.1021/acsomega.2c03016
ACS Omega 2022, 7, 44657−44669

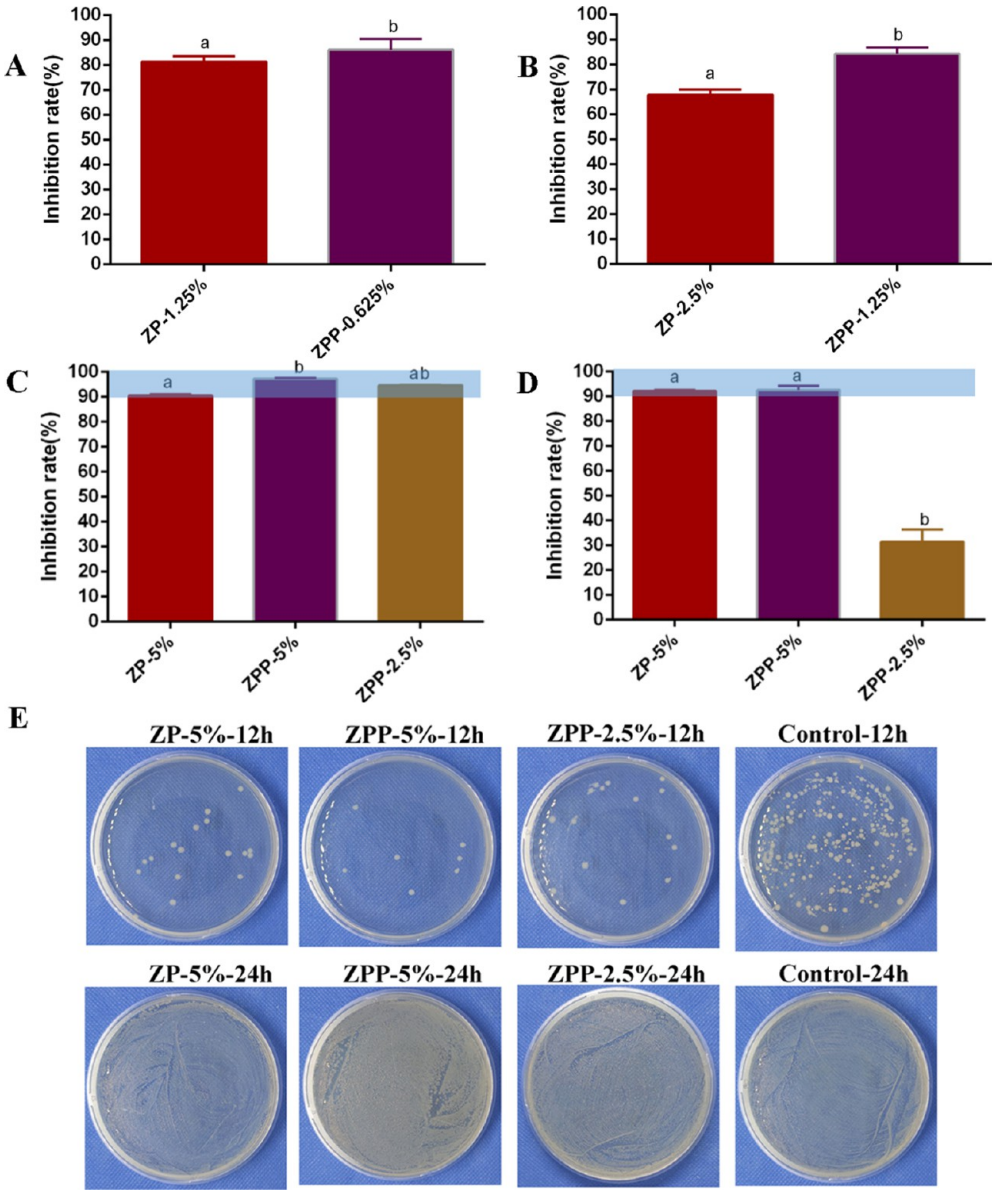

Figure 5. Inhibition rate of films to MRSA in wrapped pork samples with films at different storage points under 25 °C. (A) Inhibition rate of films to MRSA in wrapped pork samples with ZP-1.25% and ZPP-0.625% films at the point of 4 h under 25 °C. (B) Inhibition rate of films to MRSA in wrapped pork samples with ZP-2.5% and ZPP-1.25% films at the point of 6 h under 25 °C. (C) Inhibition rate of films to MRSA in wrapped pork samples with ZP-5%, ZPP-5%, and ZPP-2.5% films at the point of 12 h under 25 °C. (D) Inhibition rate of films to MRSA in wrapped pork samples with ZP-5%, ZPP-5%, and ZPP-2.5% films at the point of 24 h under 25 °C. (E) Formation of bacteria colonies: antibacterial activity of ZP-5%, ZPP-5%, ZP-2.5%, and ZPP-2.5% films at the points of 12 and 24 h under 25 °C.

Figure 3A,B, compared to the counterparts, the bacterial counts of ZP-5% and ZP-2.5% were always significantly lower than those of the blank and single PLA in the period of 4 to 120 h and 6 to 120 h. At 24 and 108 h, the bacterial counts of ZP-1.25% and ZP-0.625% were significantly lower than those of their counterparts (Figure 3C,D). Regarding ZPP, Figure 3E,F shows that the bacterial counts of ZPP-5% and ZPP-2.5% were always significantly lower than those of the blank and single PLA in the period of 6 to 120 h. In the period of 12 to 120 h, except at 72 h, the bacterial counts of ZPP-1.25% were significantly lower than those of their counterparts (Figure 3G). Nonetheless, for ZPP-0.625%, at 12 to 24 and 48 h and 108 to 120 h, the bacterial counts were significantly lower than those of the blank and PLA groups (Figure 3H). Besides, a concentration-dependent trend was observed for the bacterial counts of ZP and ZPP.

Comparison of Bacterial Counts of ZP and ZPP. To reveal the differences between the antibacterial abilities of the ZP and ZPP films, comparisons of bacterial counts at the same concentration under both 25 and 4 °C were carried out. At 25°, Figure S2A shows that the bacterial counts of ZPP-5% were significantly lower than those of the ZP-5% group in the period of 2 to 6 h ($P < 0.001$). Figure S2B shows that the bacterial counts of ZPP-2.5% were lower than that of the ZP-5% counterpart at 2 and 6 h. At concentrations of 1.25% (Figure S2C) and 0.625% (Figure S2D), the bacterial counts of the ZPP films were significantly lower than those of the ZP films at 6 and 12 h. At 4 °C, Figure S2E shows that the bacterial counts of ZPP-5% were significantly lower than those of the ZP-5% group at 36,

https://doi.org/10.1021/acsomega.2c03016
ACS Omega 2022, 7, 44657−44669

84, and 120 h ($P < 0.001$). According to Figure S2F, G, and H, in the period of 36 to 60 h, the bacterial counts of ZPP-2.5%, ZPP-1.25%, and ZPP-0.625% were significantly lower than those of their counterparts at the same time point. These results demonstrate that the antibacterial abilities of the ZPP films were better than those of the ZP films, consistent with the Zn amounts detected by ICP−MS (Table 1). It is regarded that ZnO NPs can inhibit the growth of bacteria as they induce excess reactive oxygen species. The electrostatic interactions between ZnO NPs and the cell surface may damage the membrane.[40] However, Kadiyala et al. demonstrated that ZnO NPs result in changes in energy metabolism, such as large increases in pyrimidine biosynthesis and sugar metabolism and decreases in amino acid synthesis, which could reflect a novel mechanism.[41] The ZPP films had better antibacterial effects than those of the ZP films in this study likely because of the decreased swelling ratio. Thus, less water is kept on the nanocomposites. Accordingly, the concentration of dissolved Zn^{2+} increases.[42] The dissolved Zn^{2+} has an important role in the cytotoxicity.[43] PVA could accelerate the degradation of PLA in seawater.[44] With the degradation of PLA, more ZnO NPs can be released from the films and have an antibacterial role.

Inhibition Rates of Films. As a main indicator of the bacterial effect, the inhibition rate was also evaluated. Figure 4A shows that when the temperature was 25 °C, ZP-5% was the only structure with an inhibition rate exceeding 90% at 4 and 12 h. Nevertheless, both ZPP-5% and ZPP-2.5% exhibited inhibition rates exceeding 90% at 4, 6, and 12 h (Figure 4B). At 4 °C, for the ZP films, Figure 4C shows that the inhibition rate exceeded 90% for ZP-5% in the period of 48 to 120 h and at 60 h for ZP-2.5%. Nonetheless, the inhibition rates of the ZPP films exceeded 90% at various concentrations and periods. As for ZP-5%, in the period of 48 to 120 h, the inhibition rate of ZPP-5% exceeded 90%. The inhibition rate of ZPP-2.5% exceeded 90% in the period of 48 to 60 h and 84 h and from 108 to 120 h. For ZPP-1.25%, the inhibition rate exceeded 90% in the period of 48 to 60 and 120 h. Notably, the inhibition rate of ZPP-0.625% exceeded 90% at 48 h (Figure 4D). Overall, these inhibition rates are consistent with the bacterial counts. The antibacterial results are more clearly shown in Figures 4E and S3.

Bacterial Inhibition Test on Films against MRSA at 25 °C with Different Periods. MRSA is a type of highly resistant zoonotic microorganism considered as the third most significant factor of disease worldwide among reported food-borne illnesses.[45] Many countries have reported outbreaks of livestock-associated MRSA, including Korea,[46,47] Denmark,[48] China,[49] Italy,[50] and India.[51] These pathogens are derived from many sources, including pigs, pig farmers, slaughterhouse environment,[52] open markets,[52] food products,[51] nursing homes,[53] and pork,[53,54] which increases the risk of human exposure to MRSA with toxic infections. Therefore, we investigated the antibacterial effects of nanocomposites on MRSA under the previously chosen superior conditions at 25 °C. Figure 5 shows the inhibition rates of the films against MRSA at different storage points at 25 °C. Even though the inhibition rates of ZP-1.25%, ZPP-0.625%, ZP-2.5%, and ZPP-1.25% at 4 (Figure 5A) and 6 h (Figure 5B) were lower than 90%, inhibition rates above 90% were observed when the ZP-5%, ZPP-5%, and ZPP-2.5% nanocomposites were employed in the package of pork containing MRSA at 12 (Figure 5C) and 24 h (Figure 5D). This indicates that ZPP-5% and ZPP-2.5% could inhibit the growth of MRSA at 25 °C.

Bacterial Adhesion. Figure 6 shows SEM images of the adherent MRSA on different films. The PLA films (Figure 6A)

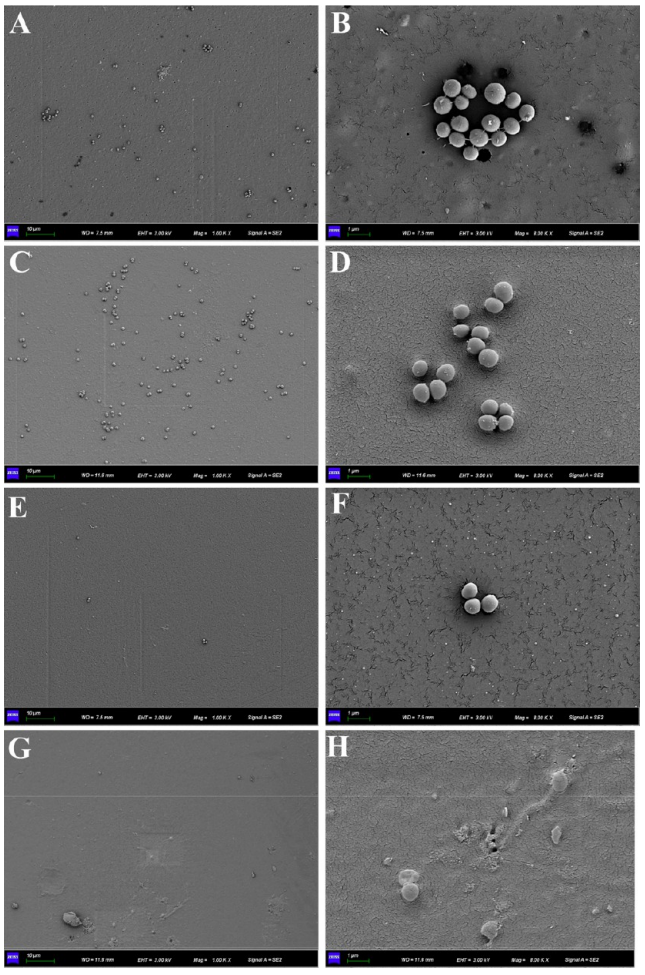

Figure 6. SEM micrographs of the films. (A) PLA (1 K), (B) PLA (8 K), (C) PVA-PLA(1 K), (D) PVA-PLA (8 K), (E) ZP-1.25% (1 K), (F) ZP-1.25%(8 K), (G) ZPP-1.25% (1 K), and (H) ZPP-1.25% (8 K).

contained many bacteria. Figure 6B (magnified view) shows that the patterns of MRSA were normal. The same result was obtained for the PVA-PLA films (Figure 6C,D). However, when ZnO NPs were added in the PLA films, the MRSA number was largely decreased (Figure 6E,F). Moreover, the coated ZnO NPs on the ZP-1.25% film could be found on the surface. On the ZPP-1.25% films, there was a low content of MRSA (Figure 6G) with a changed morphology: the original sphere shriveled up (Figure 6H), which could be a possible mechanism of the ZnO NPs antibacterial effect.

Subacute Toxicity Experiment. During the first 10 days of observation, one mouse died in each of the 400, 600, and 1000 mg/kg groups on the second day after administration, while no mice died in the other groups (Figure S4A). According to Figure S4B, the mice in the 1000 and 400 mg/kg groups lost 11% of their body weight, while the mice in the 600 and 300 mg/kg groups lost 10% of their body weight. However, the body weights of the mice in the 100 and 200 mg/kg and control groups did not exhibit a downward trend. Therefore, the maximum tolerated dose (MTD) of ZnO NPs was 200 mg/kg. According to the MTD of ZnO NPs, experimental groups with a maximum concentration of 200 mg/kg were used to evaluate the

https://doi.org/10.1021/acsomega.2c03016
ACS Omega 2022, 7, 44657−44669

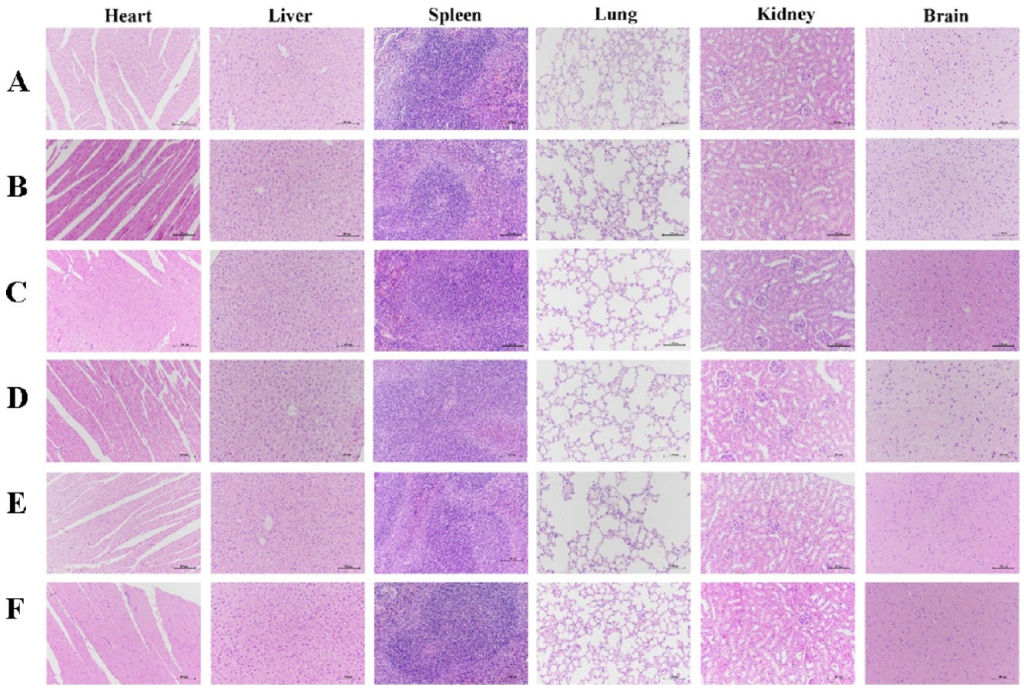

Figure 7. Histological analysis of tissues in control and ZnO NP-treated mice. ZnO NPs were given by intragastric administration to mice at different doses: (A) 0, (B) 63.3, (C) 84.4, (D) 112.5, (E) 150, and (F) 200 mg/kg, respectively. Histological section of liver, spleen, lung, and kidney stained with H&E. Data are representative of at least five mice. The scale bar is 100 μm.

oral toxicity of ZnO NPs. Within 14 days of the experiment, no death occurred in each group, and there was no considerable abnormal activity. All mice lost weight slightly on the day after administration and gradually gained weight (Figure S4C). RBC, HGB, HCT, MCV, MCH, MCHC, WBC, and PLT in routine blood assays (eight items) (Figure S5) and AST, ALT, BUN, and CREA in blood biochemical assays (four subjects) (Figure S6) were examined. Compared to the control group, there were no significant changes in the mentioned serum levels of the ZnO NP-treated groups. Furthermore, histopathological examinations were carried out to assess the toxicity of ZnO NPs with different concentrations. As illustrated in Figure 7, there were no abnormal histological and morphological changes in the main organs of livers, spleen, lung, and kidney of the ZnO NP-treated groups with doses of 63 to 200 mg/kg. Kong et al. investigated the long-term toxic effects of unmodified 50 nm ZnO NPs administered by gavage in mice and reported damages to the liver and kidney in the mice after a 90 day exposure had been discovered.[55] In this study, 10 nm ZnO NPs were used for the experiments, considerably smaller. It is of interest to evaluate the biocompatibility of ZnO NPs in various manners.

CONCLUSIONS

In this study, nanocomposite films were successfully synthesized by two methods. For the first time, we not only assessed the antibacterial effects of the ZnO nanocomposite films synthesized by the solvent evaporation method and coating methods but also employed different storage temperatures and concentrations of ZnO NPs to investigate their effects on the pork shelf life. The ZP films and ZPP films exhibited concentration-dependent antibacterial abilities. The latter exhibited better performances in extending the shelf life of pork and anti-MRSA abilities than those of the former at both 25 and 4 °C. The superior anti-bacterial abilities may be explained as ZnO NPs can decrease the bacterial adhesion and even cause bacterial rupture. The subtoxic experiment evidenced that the ZnO NPs had a lower toxicity to mice with the maximum dose of 200 mg/mL. The ZPP films are promising to extend the shelf life of pork regardless of the natural conditions or the existence of MRSA. The ZnO NPs are expected to provide remarkable contributions to antibacterial food packing.

ASSOCIATED CONTENT

Supporting Information

The Supporting Information is available free of charge at https://pubs.acs.org/doi/10.1021/acsomega.2c03016.

Comparison of bacterial counts in wrapped pork samples with the same concentration of films between ZP and ZPP films during the storage time at 25 °C and 4 °C; survival percentage of mice and body weight changes of mice after receiving ZnO NP suspension in distilled water by intragastric administration; routine blood tests of ICR mice after intragastric administration with ZnO NPs; blood chemical indexes of ICR mice after intragastric administration with ZnO NPs; and histological analysis of tissues in control and ZnO NP-treated mice (PDF)

AUTHOR INFORMATION

Corresponding Authors

Huihui Bao − *NHC Key Laboratory of Food Safety Risk Assessment, Chinese Academy of Medical Science Research Unit, China National Center for Food Safety Risk Assessment, Beijing 100022, People's Republic of China*;
Email: baohuihui@cfsa.net.cn

Tianlong Liu − *Laboratory of Veterinary Pathology and Nanopathology, College of Veterinary Medicine, China Agricultural University, Beijing 100193, People's Republic of China*; orcid.org/0000-0001-7333-9353;
Email: liutianlong@cau.edu.cn

https://doi.org/10.1021/acsomega.2c03016
ACS Omega 2022, 7, 44657−44669

Authors

Luoyan Duan − *Laboratory of Veterinary Pathology and Nanopathology, College of Veterinary Medicine, China Agricultural University, Beijing 100193, People's Republic of China; NHC Key Laboratory of Food Safety Risk Assessment, Chinese Academy of Medical Science Research Unit, China National Center for Food Safety Risk Assessment, Beijing 100022, People's Republic of China*

Feiyi Yan − *Laboratory of Veterinary Pathology and Nanopathology, College of Veterinary Medicine, China Agricultural University, Beijing 100193, People's Republic of China;* orcid.org/0000-0002-7229-252X

Lei Zhang − *NHC Key Laboratory of Food Safety Risk Assessment, Chinese Academy of Medical Science Research Unit, China National Center for Food Safety Risk Assessment, Beijing 100022, People's Republic of China*

Bo Liu − *Laboratory of Veterinary Pathology and Nanopathology, College of Veterinary Medicine, China Agricultural University, Beijing 100193, People's Republic of China*

Yichi Zhang − *Laboratory of Veterinary Pathology and Nanopathology, College of Veterinary Medicine, China Agricultural University, Beijing 100193, People's Republic of China*

Xinyuan Tian − *Laboratory of Veterinary Pathology and Nanopathology, College of Veterinary Medicine, China Agricultural University, Beijing 100193, People's Republic of China*

Zhaoping Liu − *NHC Key Laboratory of Food Safety Risk Assessment, Chinese Academy of Medical Science Research Unit, China National Center for Food Safety Risk Assessment, Beijing 100022, People's Republic of China*

Xiaodan Wang − *NHC Key Laboratory of Food Safety Risk Assessment, Chinese Academy of Medical Science Research Unit, China National Center for Food Safety Risk Assessment, Beijing 100022, People's Republic of China*

Shuaiyu Wang − *NHC Key Laboratory of Food Safety Risk Assessment, Chinese Academy of Medical Science Research Unit, China National Center for Food Safety Risk Assessment, Beijing 100022, People's Republic of China*

Jijing Tian − *NHC Key Laboratory of Food Safety Risk Assessment, Chinese Academy of Medical Science Research Unit, China National Center for Food Safety Risk Assessment, Beijing 100022, People's Republic of China*

Complete contact information is available at: https://pubs.acs.org/10.1021/acsomega.2c03016

Author Contributions

T.L. designed the study. L.D. performed the experiments and took all the photos. F.Y. wrote this article and drew the TOC. L.Z., T.L., and H.B. were responsible for the software part and analyzed the data. All authors have read, commented upon, and approved the final article.

Notes

The authors declare no competing financial interest.

■ ACKNOWLEDGMENTS

The authors acknowledge financial support from the Research and Development Projects in Key Areas of Guangdong (2019B020210002), Beijing Natural Science Foundation (6202017 and 6222022), National Key Research and Development Program of China (2018YFC1603104), and Chinese Academy of Medical Science Research Unit Program (no. 2019−12M-5-024).

■ REFERENCES

(1) Jafarzadeh, S.; Jafari, S. M.; Salehabadi, A.; Nafchi, A. M.; Uthaya Kumar, U. S. U.; Khalil, H. Biodegradable green packaging with antimicrobial functions based on the bioactive compounds from tropical plants and their by-products. *Trends Food Sci. Technol.* **2020**, *100*, 262−277.

(2) Contini, L. R. F.; Zerlotini, T. D.; Brazolin, I. F.; dos Santos, J. W. S.; Silva, M. F.; Lopes, P. S.; Sampaio, K. A.; de Carvalho, R. A.; Venturini, A. C.; Yoshida, C. M. P. Antioxidant chitosan film containing lemongrass essential oil as active packaging for chicken patties. *J. Food Process. Preserv.* **2022**, *46*(). DOI: 10.1111/jfpp.16136

(3) Bradley, E. L.; Castle, L.; Chaudhry, Q. Applications of nanomaterials in food packaging with a consideration of opportunities for developing countries. *Trends Food Sci. Technol.* **2011**, *22*, 604−610.

(4) Rezwan, K.; Chen, Q. Z.; Blaker, J. J.; Boccaccini, A. R. Biodegradable and bioactive porous polymer/inorganic composite scaffolds for bone tissue engineering. *Biomaterials* **2006**, *27*, 3413−3431.

(5) Pantani, R.; Gorrasi, G.; Vigliotta, G.; Murariu, M.; Dubois, P. PLA-ZnO nanocomposite films: Water vapor barrier properties and specific end-use characteristics. *Eur. Polym. J.* **2013**, *49*, 3471−3482.

(6) Rasal, R. M.; Janorkar, A. V.; Hirt, D. E. Poly(lactic acid) modifications. *Prog. Polym. Sci.* **2010**, *35*, 338−356.

(7) Zhang, R.; Lan, W. J.; Ji, T. T.; Sameen, D. E.; Ahmed, S.; Qin, W.; Liu, Y. W. Development of polylactic acid/ZnO composite membranes prepared by ultrasonication and electrospinning for food packaging. *LWT−Food Sci. Technol.* **2021**, *135*, 110072.

(8) Shankar, S.; Wang, L. F.; Rhim, J. W. Incorporation of zinc oxide nanoparticles improved the mechanical, water vapor barrier, UV-light barrier, and antibacterial properties of PLA-based nanocomposite films. *Mater. Sci. Eng., C* **2018**, *93*, 289−298.

(9) Jamnongkan, T.; Jaroensuk, O.; Khankhuean, A.; Laobuthee, A.; Srisawat, N.; Pangon, A.; Mongkholrattanasit, R.; Phuengphai, P.; Wattanakornsiri, A.; Huang, C. F. A Comprehensive Evaluation of Mechanical, Thermal, and Antibacterial Properties of PLA/ZnO Nanoflower Biocomposite Filaments for 3D Printing Application. *Polymers* **2022**, *14*(). DOI: 10.3390/polym14030600

(10) Kim, I.; Viswanathan, K.; Kasi, G.; Sadeghi, K.; Thanakkasaranee, S.; Seo, J. Poly(Lactic Acid)/ZnO Bionanocomposite Films with Positively Charged ZnO as Potential Antimicrobial Food Packaging Materials. *Polymers* **2019**, *11*(). DOI: 10.3390/polym11091427

(11) Kim, I.; Viswanathan, K.; Kasi, G.; Thanakkasaranee, S.; Sadeghi, K.; Seo, J. ZnO Nanostructures in Active Antibacterial Food Packaging: Preparation Methods, Antimicrobial Mechanisms, Safety Issues, Future Prospects, and Challenges. *Food Rev. Int.* **2022**, *38*, 537−565.

(12) da Silva, B. L.; Caetano, B. L.; Chiari-Andreo, B. G.; Pietro, R.; Chiavacci, L. A. Increased antibacterial activity of ZnO nanoparticles: Influence of size and surface modification. *Colloids Surf., B* **2019**, *177*, 440−447.

(13) Ding, J. J.; Hui, A. P.; Wang, W. B.; Yang, F. F.; Kang, Y. R.; Wang, A. Q. Multifunctional palygorskite@ZnO nanorods enhance simultaneously mechanical strength and antibacterial properties of chitosan-based film. *Int. J. Biol. Macromol.* **2021**, *189*, 668−677.

(14) Murariu, M.; Doumbia, A.; Bonnaud, L.; Dechief, A. L.; Paint, Y.; Ferreira, M.; Campagne, C.; Devaux, E.; Dubois, P. High-Performance Polylactide/ZnO Nanocomposites Designed for Films and Fibers with Special End-Use Properties. *Biomacromolecules* **2011**, *12*, 1762−1771.

(15) Stankovic, A.; Dimitrijevic, S.; Uskokovic, D. Influence of size scale and morphology on antibacterial properties of ZnO powders hydrothemally synthesized using different surface stabilizing agents. *Colloids Surf., B* **2013**, *102*, 21−28.

(16) Klemm, S.; Baum, M.; Qiu, H. Y.; Nan, Z. B.; Cavalheiro, M.; Teixeira, M. C.; Tendero, C.; Gapeeva, A.; Adelung, R.; Dague, E.; Castelain, M.; Formosa-Dague, C. Development of Polythiourethane/ZnO-Based Anti-Fouling Materials and Evaluation of the Adhesion of Staphylococcus aureus and Candida glabrata Using Single-Cell Force

Spectroscopy. *Nanomaterials* **2021**, *11*(). DOI: 10.3390/nano11020271
(17) De Silva, R. T.; Pasbakhsh, P.; Lee, L. S.; Kit, A. Y. ZnO deposited/encapsulated halloysite-poly (lactic acid) (PLA) nanocomposites for high performance packaging films with improved mechanical and antimicrobial properties. *Appl. Clay Sci.* **2015**, *111*, 10−20.
(18) Arfat, Y. A.; Ahmed, J.; Al Hazza, A.; Jacob, H.; Joseph, A. Comparative effects of untreated and 3-methacryloxypropyltrimethoxysilane treated ZnO nanoparticle reinforcement on properties of polylactide-based nanocomposite films. *Int. J. Biol. Macromol.* **2017**, *101*, 1041−1050.
(19) André, S.; Charton, A.; Pons, A.; Vannier, C.; Couvert, O. Viability of bacterial spores surviving heat-treatment is lost by further incubation at temperature and pH not suitable for growth. *Food Microbiol.* **2021**, *95*. DOI: 10.1016/j.fm.2020.103690
(20) Bai, X. Y.; Li, L. L.; Liu, H. Y.; Tan, L. F.; Liu, T. L.; Meng, X. W. Solvothermal Synthesis of ZnO Nanoparticles and Anti-Infection Application in Vivo. *ACS Appl. Mater. Interfaces* **2015**, *7*, 1308−1317.
(21) Sharma, V.; Singh, P.; Pandey, A. K.; Dhawan, A. Induction of oxidative stress, DNA damage and apoptosis in mouse liver after sub-acute oral exposure to zinc oxide nanoparticles. *Mutat. Res., Genet. Toxicol. Environ. Mutagen.* **2012**, *745*, 84−91.
(22) Espitia, P. J. P.; Soares, N. D. F.; Teófilo, R. F.; Coimbra, J. S. D.; Vitor, D. M.; Batista, R. A.; Ferreira, S. O.; de Andrade, N. J.; Medeiros, E. A. A. Physical-mechanical and antimicrobial properties of nanocomposite films with pediocin and ZnO nanoparticles. *Carbohydr. Polym.* **2013**, *94*, 199−208.
(23) Chu, Z. Z.; Zhao, T. R.; Li, L.; Fan, J.; Qin, Y. Y. Characterization of Antimicrobial Poly (Lactic Acid)/Nano-Composite Films with Silver and Zinc Oxide Nanoparticles. *Materials* **2017**, *10*(). DOI: 10.3390/ma10060659
(24) Annangi, B.; Rubio, L.; Alaraby, M.; Bach, J.; Marcos, R.; Hernández, A. Acute and long-term in vitro effects of zinc oxide nanoparticles. *Arch. Toxicol.* **2016**, *90*, 2201−2213.
(25) Shankar, S.; Teng, X. N.; Li, G. B.; Rhim, J. W. Preparation, characterization, and antimicrobial activity of gelatin/ZnO nanocomposite films. *Food Hydrocolloids* **2015**, *45*, 264−271.
(26) Bumbudsanpharoke, N.; Choi, J.; Park, H. J.; Ko, S. Zinc migration and its effect on the functionality of a low density polyethylene-ZnO nanocomposite film. *Food Packag. Shelf Life* **2019**, *20*, 100301.
(27) Ickrath, P.; Wagner, M.; Scherzad, A.; Gehrke, T.; Burghartz, M.; Hagen, R.; Radeloff, K.; Kleinsasser, N.; Hackenberg, S. Time-Dependent Toxic and Genotoxic Effects of Zinc Oxide Nanoparticles after Long-Term and Repetitive Exposure to Human Mesenchymal Stem Cells. *International Journal of Environmental Research and Public Health* **2017**, *14*(). DOI: 10.3390/ijerph14121590
(28) Chakartnarodom, P.; Kongkajun, P.; Senthongkaew, N. *Application of Numerical Method and Statistical Analysis in the Integrated Intensity Calculation of the Peaks from the X-Ray Diffraction (XRD) Pattern of α-Iron* ; Trans Tech Publications Ltd, 2015; Vol. *659*, pp 350−354.
(29) Wardana, A. A.; Suyatma, N. E.; Muchtadi, T. R.; Yaliani, S. Influence of ZnO nanoparticles and stearic acid on physical, mechanical and structural properties of cassava starch-based bionanocomposite edible films. *Int. Food Res. J.* **2018**, *25*, 1837−1844.
(30) Yu, F. Y.; Fei, X.; He, Y. Q.; Li, H. Poly(lactic acid)-based composite film reinforced with acetylated cellulose nanocrystals and ZnO nanoparticles for active food packaging. *Int. J. Biol. Macromol.* **2021**, *186*, 770−779.
(31) Kirschner, M. R. C.; Rippel, T.; Ternus, R.; Duarte, G. W.; Riella, H. G.; Dal Magro, J.; Mello, J. M. M.; Silva, L. L.; Fiori, M. A. Antibacterial polyamide obtained by the incorporation of glass microparticles doped with ionic zinc and by zinc oxide nanoparticle: Evaluation with Salmonella typhimurium and Staphylococcus aureus. *J. Appl. Polym. Sci.* **2017**, *134*(). DOI: 10.1002/app.45005
(32) Heydari-Majd, M.; Ghanbarzadeh, B.; Shahidi-Noghabi, M.; Najafi, M. A.; Adun, P.; Ostadrahimid, A. Kinetic release study of zinc from polylactic acid based nanocomposite into food simulants. *Polym. Test.* **2019**, *76*, 254−260.
(33) Xiao, X.; Zhang, X.; Yang, S.; Zhao, C. STUDY ON MIGRATION BEHAVIOR OF NANO-SELENIUM PARTICLES OF NANO-SELENIUM PACKAGING MATERIALS IN FOOD SIMULANTS. *Digest Journal of Nanomaterials and Biostructures* **2018**, *13*, 427−437.
(34) Lu, W. W.; Jiang, K.; Chu, Z. Z.; Yuan, M. L.; Tang, Z. Y.; Qin, Y. Y. Changes of thermal properties and microstructure of nano-ZnO/polylactic acid composite films during Zn migration. *Packag. Technol. Sci.* **2021**, *34*, 3−10.
(35) Huang, H.; Li, L.; Qin, Y.; Luo, Z.; Chen, H.; Ru, Q. Migration rules of Zn from nano-ZnO modified LDPE food packaging films. *Nongye Gongcheng Xuebao/Transactions of the Chinese Society of Agricultural Engineering* **2018**, *34*, 278−283283.
(36) Lee, J.; Bhattacharyya, D.; Easteal, A. J.; Metson, J. B. Properties of nano-ZnO/poly(vinyl alcohol)/poly(ethylene oxide) composite thin films. *Curr. Appl. Phys.* **2008**, *8*, 42−47.
(37) Fortunati, E.; Rinaldi, I.; Peltzer, J. M.; Bloise, S.; Visai, L.; Armentano, M.; Jiménez, A.; Latterini, N.; Kenny, L. Nanobiocomposite films with modified cellulose nanocrystals and synthesized silver nanoparticles. *Carbohydr. Polym.* **2014**, *101*, 1122−1133.
(38) Fukushima, K. Poly(trimethylene carbonate)-based polymers engineered for biodegradable functional biomaterials. *Biomater. Sci.* **2016**, *4*, 9−24.
(39) Sporchia, F.; Kebreab, E.; Caro, D. Assessing the multiple resource use associated with pig feed consumption in the European Union. *Sci. Total Environ.* **2021**, *759*, 144306.
(40) Li, Y.; Zhang, W.; Niu, J. F.; Chen, Y. S. Mechanism of Photogenerated Reactive Oxygen Species and Correlation with the Antibacterial Properties of Engineered Metal-Oxide Nanoparticles. *Acs Nano* **2012**, *6*, 5164−5173.
(41) Kadiyala, U.; Turali-Emre, E. S.; Bahng, J. H.; Kotov, N. A.; VanEpps, J. S. Unexpected insights into antibacterial activity of zinc oxide nanoparticles against methicillin resistant Staphylococcus aureus (MRSA). *Nanoscale* **2018**, *10*, 4927−4939.
(42) Swaroop, K.; Somashekarappa, H. M. In vitro Biocompatibility and Antibacterial Activity of Gamma Ray Crosslinked ZnO/PVA Hydrogel Nanocomposites. *Mater. Today Proc.* **2018**, *5*, 21314−21321.
(43) Song, W.; Zhang, J.; Guo, J.; Zhang, L.; Ding, Z.; Li, J.; Sun, F. Role of the dissolved zinc ion and reactive oxygen species in cytotoxicity of ZnO nanoparticles. *Toxicol. Lett.* **2010**, *199*, 389−397.
(44) Huang, D.; Hu, Z. D.; Liu, T. Y.; Lu, B.; Zhen, Z. C.; Wang, G. X.; Ji, J. H. Seawater degradation of PLA accelerated by water-soluble PVA. *E-Polymers* **2020**, *20*, 759−772.
(45) Ramanathan, S.; Arunachalam, K.; Shi, C.; Lin, X. Marine Bacterial Secondary Metabolites: A Treasure House for Structurally Unique and Effective Antimicrobial Compounds. *Mar. Drugs* **2021**, *19*, 530.
(46) Back, S. H.; Eom, H. S.; Lee, H. H.; Lee, G. Y.; Park, S. J.; Yang, K. T. Livestock-associated methicillin-resistant Staphylococcus aureus in Korea: Antimicrobial resistance and molecular characteristics of LA-MRSA strains isolated from pigs, pig farmers, and farm environment. *J. Vet. Sci.* **2020**, *21*(). DOI: 10.4142/jvs.2020.21.e2
(47) Chung, H. Y.; Kim, Y.-T.; Kwon, J.-G.; Im, H. H.; Ko, D.; Lee, J.-H.; Choi, S. H. Molecular interaction between methicillin-resistant Staphylococcus aureus (MRSA) and chicken breast reveals enhancement of pathogenesis and toxicity for food-borne outbreak. *Food Microbiol.* **2021**, *93*, 103602.
(48) Li, H.; Ingmer, H.; Staubrand, N.; Dalsgaard, A.; Leisner, J. J.; Andersen, P. S.; Stegger, M.; Sieber, R. N. Antimicrobial Resistance and Virulence Gene Profiles of Methicillin-Resistant and -Susceptible Staphylococcus aureus From Food Products in Denmark. *Front. Microbiol.* **2019**, *10*. DOI: 10.3389/fmicb.2019.02681
(49) Liu, M.; Feng, K.; Yang, Y.; Cao, J.; Zhang, J.; Xu, X.; Hernández, M.; Wei, M.; Fan, S. H. Transcriptomic and metabolomic analyses reveal antibacterial mechanism of astringent persimmon tannin against Methicillin-resistant Staphylococcus aureus isolated from pork. *Food Chem.* **2020**, *309*. DOI: 10.1016/j.foodchem.2019.125692

(50) Normanno, G.; Dambrosio, P.; Lorusso, A.; Samoilis, V.; Di Taranto, G.; Parisi, A. Methicillin-resistant Staphylococcus aureus (MRSA) in slaughtered pigs and abattoir workers in Italy. *Food Microbiol.* **2015**, *51*, 51−56.
(51) Zehra, A.; Gulzar, R.; Singh, S.; Kaur, M.; Gill, J. P. S. Prevalence, multidrug resistance and molecular typing of methicillin-resistant Staphylococcus aureus (MRSA) in retail meat from Punjab, India. *J. Global Antimicrob. Resist.* **2019**, *16*, 152−158.
(52) Ivbule, M.; Miklaševičs, E.; Čupāne, L.; Bērziņa, L.; Bālinš, A.; Valdovska, A. Presence of methicillin-resistant Staphylococcus aureus in slaughterhouse environment, pigs, carcasses, and workers. *J. Vet. Res.* **2017**, *61*, 267−277.
(53) Liu, M. M.; Feng, M. X.; Yang, K.; Cao, Y. F.; Zhang, J.; Xu, J. N.; Hernandez, S. H.; Wei, X. Y.; Fan, M. T. Transcriptomic and metabolomic analyses reveal antibacterial mechanism of astringent persimmon tannin against Methicillin-resistant Staphylococcus aureus isolated from pork. *Food Chem.* **2020**, *309*. DOI: 10.1016/j.foodchem.2019.125692
(54) Schoen, M. E.; Peckham, T. K.; Shirai, J. H.; Kissel, J. C.; Thapaliya, D.; Smith, T. C.; Meschke, J. S. Risk of nasal colonization of methicillin-resistant Staphylococcus aureus during preparation of contaminated retail pork meat. *Microb. Risk Anal.* **2020**, *16*. DOI: 10.1016/j.mran.2020.100136
(55) Kong, T.; Zhang, S. H.; Zhang, C.; Zhang, J. L.; Yang, F.; Wang, G. Y.; Yang, Z. J.; Bai, D. Y.; Zhang, M. Y.; Wang, J.; Zhang, B. H. Long-Term Effects of Unmodified 50nm ZnO in Mice. *Biol. Trace Elem. Res.* **2019**, *189*, 478−489.

https://doi.org/10.1021/acsomega.2c03016
ACS Omega 2022, 7, 44657−44669